



CHORUS

This is the accepted manuscript made available via CHORUS. The article has been published as:

Scalable continuous-variable entanglement of optical fields via concurrent interactions with separated atomic ensembles

Hong Sun and Xiangming Hu

Phys. Rev. A **85**, 032320 — Published 19 March 2012

DOI: [10.1103/PhysRevA.85.032320](https://doi.org/10.1103/PhysRevA.85.032320)

Scalable continuous variable entanglement of optical fields via concurrent interactions with separated atomic ensembles

Hong Sun and Xiangming Hu*

School of Physical Science and Technology, Central China Normal University, Wuhan 430079, People's Republic of China

It has been known that one reservoir of driven two-level atoms can establish two-mode interactions and generate bipartite continuous-variable entangled light. Here we show that three-mode interactions can be created by combining two such reservoirs, each of which interacts with two adjacent fields in frequency. It is shown that the van Loock-Furusawa criteria [Phys. Rev. A 67, 052315 (2003)] are well satisfied for a wide range of the relevant parameters. This determines that tripartite continuous variable Greenberger-Horne-Zeilinger entanglement is obtainable. The scalability to more fields is straightforward, allowing an alternative implementation of a multipartite quantum networks with continuous variables.

PACS numbers: 03.67.Bg, 42.50.Pq, 42.50.Dv, 32.80.Qk

I. INTRODUCTION

Continuous variable (CV) entanglement has great potential in quantum networks and information processing [1]. Possible applications range from quantum teleportation [2–6] to controlled dense coding [7] and secret sharing [8]. The simplest teleportation schemes rely on bipartite entanglement. However, more sophisticated protocols may require entanglement of three parts or more [9–12]. Greenberger-Horne-Zeilinger (GHZ) state is one of important types of genuine multiple entanglement. In particular, the tripartite CV GHZ state [13] is a three-mode momentum (position) eigenstate with total momentum $p_1 + p_2 + p_3 = 0$ (total position $x_1 + x_2 + x_3 = 0$) and relative positions $x_i - x_j = 0$ (relative momenta $p_i - p_j = 0$), $i, j = 1, 2, 3$, $i \neq j$, and exhibits maximum entanglement. Experimental progresses have been made by using independent squeezed fields and beam splitters [9–12].

In the context of cavity quantum electrodynamics, the atom-field interactions are fundamental mechanisms for creating the multipartite entanglement without use of initially prepared squeezing. Typically, there are three kinds of related systems as follows for the generation of two-mode CV entanglement. The first one is a two-photon correlated emission laser, where the laser gain and the quantum correlation are established by combining Raman and EIT (electromagnetically induced transparency [14–18]) interactions [19–21] in Lambda systems. For this case, CV entanglement is compatible with large numbers of photons in the two modes. The second kind of systems is to use dispersive interactions of atoms with both the driving and cavity fields to create parametric conversion [22, 23]. In this way one can obtain a two-mode squeeze operator and thus the Einstein-Podolsky-Rosen entangled light [24]. The third kind of schemes is based on the wave-mixing interactions in near-resonant systems. Typically, two-level atoms are used for this pur-

pose [25, 26]. The new photons are emitted into the cavity modes simultaneously when the atoms absorb two photons from the strong driving field. The frequencies of the cavity fields are determined by Rabi resonances. The common essence in the above three different kinds of systems is the two-photon process, which is responsible for the desired quantum correlations.

To obtain multipartite entanglement, it seems that one has to resort to multilevel atomic systems [27–35], which are usually driven by two or more strong fields. On one hand, the strong driving fields could cause cross couplings between adjacent transitions in frequency. The cross couplings lead to not only Stark shift but also remarkable phase damping [16, 36]. This damping will spoil the desirable quantum correlations. On the other hand, the dressed multilevel atomic systems generally have closely spaced dressed states, which gives rise to a difficulty in separating Rabi resonances. At the same time, the coupling of the cavity fields to the adjacent dressed transitions will play an opposite role in creating the desired quantum correlations.

Here we propose an alternative scalable scheme for concurrent interactions and multipartite GHZ entanglement. In the present work, we focus on the case where three cavity fields interact with two atomic ensembles. Each ensemble is only driven by one external field and is coupled to two weak cavity fields of adjacent frequencies. By using the van Loock-Furusawa [37] criteria we examine the three-mode correlations. The results show that GHZ entanglement can be achieved. The present scheme have three advantages as follows. First, GHZ Entanglement is generated without the use of the initial squeezed states. All field components are amplified from the vacuum fields, unlike those that use initially squeezed fields [9–12]. Second, each atomic ensemble is driven by a single driving field, and the crossing couplings on the adjacent transitions are greatly reduced. Last but not the least, this scheme is more easily scalable to multimode systems.

The remaining parts of the present paper are organized as follows. In Sec. II, we describe our model and derive the master equation. In Sec. III, we calculate the correlations of the three fields and examine whether tripartite

*Corresponding author. Email: xmhu@phy.ccnu.edu.cn.

entanglement criteria are satisfied. In Sec. IV, we give realistic considerations of our proposal. A summary is given in Sec. V.

II. MODEL AND MASTER EQUATION

Our scheme uses two ensembles of two-level atoms in an optical cavity, as shown in Fig. 1. The atoms are cooled in a standard magneto-optical trap [38, 39]. Ensemble j consists of N_j atoms and is driven by one external field, $j = 1, 2$. Three cavity fields are generated, which are described by annihilation and creation operators a_l and a_l^\dagger , $l = 1, 2, 3$. The fields $a_{1,3}$ are coupled to the two different atomic ensembles 1 and 2, respectively, while the field a_2 is coupled to both ensembles. The atoms in two different ensembles have different but near resonance frequencies. Fig. 2 shows the frequency positions of the atoms $\bar{\omega}_{1,2}$, the applied fields $\omega_{1,2}$, and the cavity fields $\nu_{1,2,3}$. In the rotating wave approximation and in an appropriate rotating frame, we derive the master equation for the density operator ρ of the atom-field composite system as [40]

$$\dot{\rho} = -\frac{i}{\hbar}[H, \rho] + \mathcal{L}\rho, \quad (1)$$

with the Hamiltonian $H = H_0 + H_1$, where

$$H_0 = \sum_{j=1}^2 \sum_{\mu_j=1}^{N_j} \hbar[\Delta_j \sigma_{11}^{\mu_j} + \frac{\Omega_j}{2}(\sigma_{10}^{\mu_j} + \sigma_{01}^{\mu_j})], \quad (2)$$

describes the interaction of the driving fields with the atoms, and

$$H_1 = \sum_{j=1}^2 \sum_{\mu_j=1}^{N_j} \hbar \sigma_{10}^{\mu_j} (g_-^{(j)} a_j e^{-i\Delta_-^{(j)} t} + g_+^{(j)} a_{j+1} e^{-i\Delta_+^{(j)} t}) + \text{H.c.}, \quad (3)$$

represents the interaction of the cavity fields with atoms. Here H.c. is the Hermitian conjugate. For the μ_j -th atom, $\sigma_{\alpha\beta}^{\mu_j} = |\alpha\rangle_{\mu_j} \langle\beta|$ ($\alpha, \beta = 0, 1$) are the atomic spin-flip operators when $\alpha \neq \beta$ and the projection operators when $\alpha = \beta$. $\Delta_j = \bar{\omega}_j - \omega_j$ is the detuning between the atomic ensemble j and the driving field j , and $\Delta_+^{(j)} = \nu_{j+1} - \omega_j$ ($\Delta_-^{(j)} = \nu_j - \omega_j$) denotes the detuning between the applied field j and the higher (lower) sideband. Ω_j is the Rabi frequency and is assumed to be real. $g_+^{(j)}$ ($g_-^{(j)}$) is the coupling strength between the atomic ensemble j and the higher (lower) sideband. The decay term in Eq. (1) takes the form $\mathcal{L}\rho = \mathcal{L}_a\rho + \mathcal{L}_c\rho$, where

$$\mathcal{L}_a\rho = \sum_{j=1}^2 \sum_{\mu_j=1}^{N_j} \frac{\gamma_j}{2} \mathcal{D}[\sigma_{01}^{\mu_j}]\rho, \quad (4)$$

denotes the atomic relaxation, and

$$\mathcal{L}_c\rho = \sum_{l=1}^3 \frac{\kappa_l}{2} \mathcal{D}[a_l]\rho, \quad (5)$$

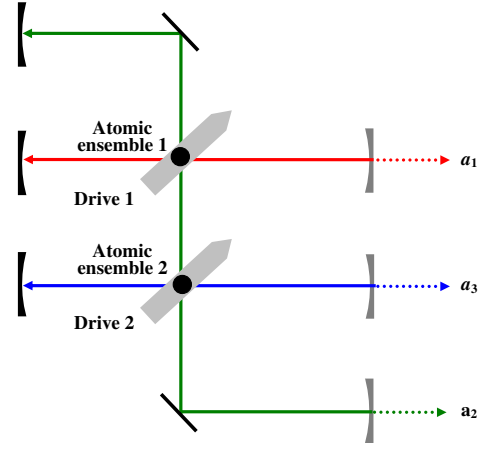


FIG. 1: (Color online) Possible cavity setup. Two atomic ensembles are respectively driven by two strong fields and three cavity fields $a_{1,2,3}$ are generated.

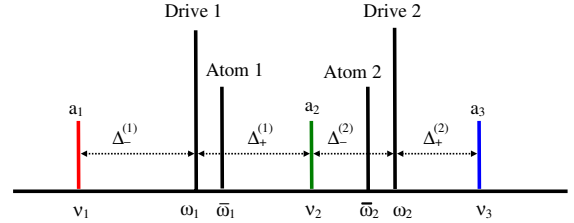


FIG. 2: (Color online) Frequencies of the atoms $\bar{\omega}_{1,2}$, the applied fields $\omega_{1,2}$, and the cavity fields $\nu_{1,2,3}$.

stands for the cavity loss. We have defined superoperator $\mathcal{D}[Q]\rho \equiv [Q\rho, Q^\dagger] + [Q, \rho Q^\dagger]$ for an operator Q . γ 's and κ 's represent the atomic spontaneous decay rates and the cavity decay rates, respectively.

It becomes aware that in the presence of only the atomic ensemble 1, an atom absorbs two photons from

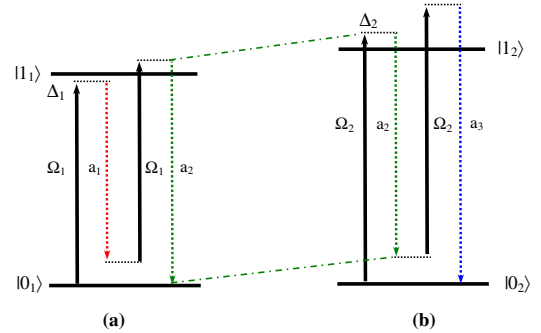


FIG. 3: (Color online) Atomic transitions due to the driving fields and the cavity fields (a) for ensemble 1 and (b) for ensemble 2.

the driving field 1 and then emits two sideband photons, as shown in Fig. 3 (a). Through two-photon process, entanglement is created between the two sidebands a_1 and a_2 . The case is the same for the presence of only the atomic ensemble 2 (as shown Fig. 3(b)), and a_2 and a_3 is entangled with each other. At present, we combine the above two cases. The field a_2 is coupled simultaneously to the two atomic ensembles. It is expected that three cavity fields are correlated via the concurrent interactions.

We diagonalize the Hamiltonian H_0 for the interaction of the driving fields with two atomic ensembles to show the resonant interactions of the cavity fields with the atoms [41]. For the j -th atomic ensemble, the dressed states are obtained as

$$\begin{aligned} |+\rangle_j &= s_j|0\rangle_j + c_j|1\rangle_j, \\ |-\rangle_j &= c_j|0\rangle_j - s_j|1\rangle_j, \end{aligned} \quad (6)$$

where $s_j = \sqrt{\frac{1}{2} - \frac{\delta_j}{2\sqrt{1+\delta_j^2}}}$, $c_j = \sqrt{1 - s_j^2}$, and $\delta_j = \frac{\Delta_j}{\Omega_j}$ are defined as the normalized detunings, $j = 1, 2$. The dressed-states $|\pm\rangle_j$ have eigenvalues $\lambda_{\pm}^{(j)} = \frac{1}{2}(\Delta_j \pm d_j)$, where we have used the generalized Rabi frequencies $d_j = \sqrt{\Delta_j^2 + \Omega_j^2}$. Then the free Hamiltonian simplifies to $H_0 = \sum_{j=1}^2 \sum_{\mu_j=1}^{N_j} \hbar(\lambda_+^{(j)} \sigma_{++}^{\mu_j} + \lambda_-^{(j)} \sigma_{--}^{\mu_j})$, where $\sigma_{\pm\pm}^{\mu_j} = |\pm\rangle_{\mu_j} \langle \pm|$. We assume the driving fields to be strong ($d_j \gg \gamma_j$) and the cavity fields to be resonant with the Rabi sidebands $\Delta_+^{(j)} = -\Delta_-^{(j)} = d_j$ [42, 43]. After applying a unitary transformation $U = \exp(-iH_0t/\hbar)$ and neglecting the rapidly oscillating factors $\exp(\pm id_j t)$ and $\exp(\pm 2id_j t)$, we rewrite the Hamiltonian for the interaction of the cavity fields with the two atomic ensembles as

$$H_1 = \sum_{j=1}^2 \sum_{\mu_j=1}^{N_j} \hbar \sigma_{+-}^{\mu_j} (g_-^{(j)} c_j^2 a_j - g_+^{(j)} s_j^2 a_{j+1}^\dagger) + \text{H.c.} \quad (7)$$

Correspondingly, the atomic damping term becomes

$$\begin{aligned} \mathcal{L}_a \rho &= \sum_{j=1}^2 \sum_{\mu_j=1}^{N_j} \frac{\gamma_j}{2} \{ c_j^4 \mathcal{D}[\sigma_{-+}^{\mu_j}] \rho + s_j^4 \mathcal{D}[\sigma_{+-}^{\mu_j}] \rho \\ &\quad + c_j^2 s_j^2 \mathcal{D}[\sigma_{++}^{\mu_j} - \sigma_{--}^{\mu_j}] \rho \}. \end{aligned} \quad (8)$$

We assume that the cavity relaxation times κ_l^{-1} ($l = 1, 2, 3$) are much larger than the atomic relaxation times γ_j^{-1} ($j = 1, 2$). Then we can work in the adiabatic approximation and eliminate the atomic variables from the coupled system [40]. In the linear theory [40, 43], the cavity fields do not change the atomic populations. The equation for the dressed populations $P_j^\pm = (1/N_j) \sum_{\mu_j=1}^{N_j} \langle \sigma_{\pm\pm}^{\mu_j} \rangle$ is derived as

$$\dot{P}_j^\pm = \gamma_j s_j^4 P_j^- - \gamma_j c_j^4 P_j^+, \quad (9)$$

together with the closure relation $P_j^+ + P_j^- = 1$. At the steady state we have the dressed populations

$$P_j^+ = \frac{s_j^4}{c_j^4 + s_j^4}, \quad P_j^- = \frac{c_j^4}{c_j^4 + s_j^4}. \quad (10)$$

Finally the master equation for the cavity fields is obtained as

$$\begin{aligned} \dot{\rho} &= \frac{1}{2} \sum_{l=1}^3 \{ \lambda_l [a_l^\dagger \rho, a_l] + (\xi_l + \kappa_l) [a_l \rho, a_l^\dagger] \} \\ &\quad - \frac{1}{2} \sum_{j=1}^2 \{ \chi_{j,j+1} ([a_j \rho, a_{j+1}] + [a_j, \rho a_{j+1}]) \\ &\quad + \chi_{j+1,j} ([a_{j+1} \rho, a_j] + [a_{j+1}, \rho a_j]) \} + \text{H.c.}, \end{aligned} \quad (11)$$

where the λ_l ($l = 1, 2, 3$) terms together with their Hermitian conjugates indicate the gain to the cavity mode a_l due to the medium, the ξ_l terms together with their Hermitian conjugates represent the absorption, and the $\chi_{j,j+1}$ and $\chi_{j+1,j}$ ($j = 1, 2$) terms together with their Hermitian conjugates describe the crossing couplings between the cavity fields j and $j+1$. These parameters read as $\lambda_1 = c_1^4 A_1^- P_1^+$, $\lambda_2 = s_1^4 A_1^+ P_1^- + c_2^4 A_2^- P_2^+$, $\lambda_3 = s_2^4 A_2^+ P_2^-$, $\xi_1 = c_1^4 A_1^- P_1^-$, $\xi_2 = s_1^4 A_1^+ P_1^+ + c_2^4 A_2^- P_2^-$, $\xi_3 = s_2^4 A_2^+ P_2^+$, $\chi_{12} = c_1^2 s_1^2 B_1 P_1^-$, $\chi_{21} = c_1^2 s_1^2 B_1 P_1^+$, $\chi_{23} = 2c_2^2 s_2^2 B_2 P_2^-$, $\chi_{32} = c_2^2 s_2^2 B_2 P_2^+$, $A_j^\pm = 2|g_\pm^{(j)}|^2 N_j \Gamma_j^{-1}$, $B_j = 2g_+^{(j)} g_-^{(j)} N_j \Gamma_j^{-1}$, and $\Gamma_j = \gamma_j (\frac{1}{2} + c_j^2 s_j^2)$. In what follows we will show that the cross coupling terms are responsible for tripartite entanglement.

III. FIELD CORRELATIONS AND INSEPARABILITY

Here we will demonstrate genuine tripartite entanglement in our system. To do this we follow the standard techniques [44] and calculate the correlation of the generated fields. Choosing the normal order $a_1^\dagger, a_2^\dagger, a_3^\dagger, a_1, a_2, a_3$, using the generalized P representation [45], and defining the corresponding c -number variables $\alpha_1^\dagger, \alpha_2^\dagger, \alpha_3^\dagger, \alpha_1, \alpha_2, \alpha_3$, we derive the Langevin equations from the master equation (11) as

$$\begin{aligned} \dot{\alpha}_1 &= \tilde{\lambda}_1 \alpha_1 + \tilde{\chi}_{12} \alpha_2^\dagger + F_{\alpha_1}, \\ \dot{\alpha}_2 &= \tilde{\lambda}_2 \alpha_2 - \tilde{\chi}_{12} \alpha_1^\dagger + \tilde{\chi}_{23} \alpha_3^\dagger + F_{\alpha_2}, \\ \dot{\alpha}_3 &= \tilde{\lambda}_3 \alpha_3 - \tilde{\chi}_{23} \alpha_2^\dagger + F_{\alpha_3}, \end{aligned} \quad (12)$$

together with those equations for $\alpha_1^\dagger, \alpha_2^\dagger$ and α_3^\dagger . Here we have used the parameters $\tilde{\lambda}_l = \frac{1}{2}(\lambda_l - \xi_l - \kappa_l)$ and $\tilde{\chi}_{jk} = \frac{1}{2}(\chi_{jk} - \chi_{kj})$ for conciseness, $l, j, k = 1, 2, 3, j < k$. The fluctuating terms have the vanishing means $\langle F_x(t) \rangle = 0$ and the white noise correlations $\langle F_x(t) F_y(t') \rangle = D_{xy} \delta(t - t')$. The nonvanishing diffusion coefficients are $D_{\alpha_1^\dagger \alpha_1} = \lambda_1$, $D_{\alpha_2^\dagger \alpha_2} = \lambda_2$, $D_{\alpha_3^\dagger \alpha_3} = \lambda_3$, $D_{\alpha_1 \alpha_2} = \frac{1}{2}(\chi_{12} + \chi_{21})$, and

$D_{\alpha_2\alpha_3} = \frac{1}{2}(\chi_{23} + \chi_{32})$, and $D_{xy} = D_{yx}$, $D_{y^\dagger x^\dagger} = D_{xy}^\dagger$. Arranging the field variables together in the vector $R = (\alpha_1, \alpha_2, \alpha_3, \alpha_1^\dagger, \alpha_2^\dagger, \alpha_3^\dagger)^T$ and writing $\delta R = R - \langle R \rangle$, we obtain the linearized Langevin equations as

$$\frac{d}{dt}\delta R(t) = -G\delta R(t) + F(t), \quad (13)$$

where the drift matrix G can easily be obtained from Eq. (12). The correlation matrix for the noise term $\langle F(t)F^T(t') \rangle = D\delta(t-t')$ is easily obtained from the above diffusion coefficients. The system reaches its steady state and is stable when all of the eigenvalues of G have positive real parts. The linearised Langevin equations (13) can be rewritten in terms of frequency spectrum, which is defined by $\delta R(\omega) = \frac{1}{\sqrt{2\pi}} \int dt e^{-i\omega t} \delta R(t)$. Thus we can calculate the correlation spectrum $\langle \delta R(\omega) \delta R^T(\omega') \rangle = S(\omega) \delta(\omega + \omega')$, where

$$S(\omega) = (G - i\omega I)^{-1} D (G^T + i\omega I)^{-1}. \quad (14)$$

Here we are interested in the case where the density matrix is not separable in any form, i.e., the tripartite CV GHZ-type states. We use a set of conditions to investigate the presence of entanglement in this system, which was put forward by van Loock and Furusawa [37]. The guaranty of any two of the following inequalities is sufficient to demonstrate true CV tripartite entanglement

$$V_{jk} = \langle [\delta(X_j^o - X_k^o)]^2 \rangle + \langle [\delta(Y_j^o + Y_k^o + f_l Y_l^o)]^2 \rangle < 4, \quad (15)$$

where $j, k, l = 1, 2, 3$, $j < k \neq l$. We have defined the position and momentum operators $X_l^o = a_l^{out} + a_l^{\dagger out}$ and $Y_l^o = -i(a_l^{out} - a_l^{\dagger out})$ for the output fields a_l^{out} , which relate to the intracavity fields a_l and the input fields a_l^{in} through the relations [44]: $a_l^{in} + a_l^{out} = \sqrt{\kappa_l} a_l$. The factors f_l are arbitrary real numbers to minimize the variances in Eq. (15) and are calculated as

$$f_l = -\frac{\langle \delta Y_j^o \delta Y_l^o \rangle + \langle \delta Y_k^o \delta Y_l^o \rangle}{\langle (\delta Y_l^o)^2 \rangle}. \quad (16)$$

Here we use the vacuum inputs and derive the spectra of the output fields $V_{jk}(\omega)$. The required auto-correlation spectra and cross-correlation spectra are, respectively,

$$\begin{aligned} \langle (\delta X_j^o)^2 \rangle(\omega) &= \langle (\delta Y_j^o)^2 \rangle(\omega) \\ &= 1 + \kappa_j \langle (\delta X_j)^2 \rangle(\omega), \end{aligned} \quad (17)$$

and

$$\begin{aligned} \langle \delta X_j^o \delta X_k^o \rangle(\omega) &= (-1)^{j-k} \langle \delta Y_j^o \delta Y_k^o \rangle(\omega) \\ &= \sqrt{\kappa_j \kappa_k} \langle \delta X_j \delta X_k \rangle(\omega), \end{aligned} \quad (18)$$

where we have used the expressions $\langle (\delta X_j^o)^2 \rangle(\omega) \delta(\omega + \omega') = \langle \delta X_j^o(\omega) \delta X_j^o(\omega') \rangle$, $\langle \delta X_j^o \delta X_k^o \rangle(\omega) \delta(\omega + \omega') = \langle \delta X_j^o(\omega) \delta X_k^o(\omega') \rangle$ ($j, k = 1, 2, 3; j \neq k$), and the similar expressions for the position operators $X_j = a_j + a_j^\dagger$ of the intracavity fields a_j .

So far we get the measurable spectral quantities outside the cavity $V_{jk}(\omega)$. In what follows we present the numerical results as follows. We assume that $g_+^{(j)} = g_-^{(j)} = g_j$ ($j = 1, 2$) and rescale the decay rates in units of γ_1 . Cooperativity parameters are defined as $C_j = \frac{|g_j|^2 N_j}{\gamma_j^2}$. In Fig. 4 we plot the output zero frequency spectra $V_{jk}(0)$ as functions of the normalized detuning δ_1 for (a,b) $\delta_2 = \pm 0.2$, (c,d) $\delta_2 = \pm 0.5$, (e) $\delta_2 = 1$, and (f) $\delta_2 = -2$. The other parameters are $\gamma_{1,2} = 1$, $\kappa_{1,2,3} = 0.1$, $C_{1,2} = 20$. We see from this figure that for various values of the normalized detuning δ_2 , there are wide ranges of the normalized detuning δ_1 where at least two of the correlations are below 4. Any two correlations falling below 4 are sufficient for the occurrence of tripartite GHZ entanglement. Due to the symmetry of the system, if we exchange δ_1 and $-\delta_2$, the curves V_{12} and V_{23} will interchange. In fact $V_{12} = V_{23}$ at $\delta_1 = -\delta_2$ is a signature of this feature.

In Fig. 5 we show the correlation spectra for different parameters. For the sake of comparison we have taken Fig. 4(d) as an example, which is re-plotted in (a). (b) is for different cooperativity parameters $C_1 = 10$, $C_2 = 20$, (c) is for the different rates of atomic decay $\gamma_1 = 1$, $\gamma_2 = 5$, and (d) is for different rates of cavity loss $\kappa_1 = 0.1$, $\kappa_2 = 0.15$, $\kappa_3 = 0.2$. In (b,c,d), the other parameters are chosen the same as in (a). We clearly see that the correlation spectra are insensitive to various parameters. This means that the above GHZ entanglement is achievable for a wide range of parameters.

From the master equation (11) (or the Langevin equations Eqs. (12)), we can see that the above nonclassical correlations are attributed to the crossing couplings described by the χ terms. These terms that cause the correlation $\langle \delta \alpha_1(\omega) \delta \alpha_2(-\omega) \rangle$ ($\langle \delta \alpha_2(\omega) \delta \alpha_3(-\omega) \rangle$) in Eq. (18) originates from the absorption of two photons from the driving fields and the emission of two sideband photons into the cavity fields. For the atomic ensemble 1, an atom absorbs two photons from the driving field 1 and then emits two sideband photons, as shown in Fig. 3 (a). Through two-photon process, entanglement is created between the two sidebands a_1 and a_2 . Similarly, for the atomic ensemble 2 (as shown Fig. 3(b)), a_2 and a_3 is entangled with each other. Our case combines the above two ensembles. The field a_2 is coupled simultaneously to the two atomic ensembles. This plays a crucial role in the correlations between the three modes $a_{1,2,3}$. By virtue of the connecting action of a_2 , quantum correlations between the indirect-coupling cavity fields a_1 and a_3 can also be established ($\langle \delta \alpha_1(\omega) \delta \alpha_3^\dagger(-\omega) \rangle \neq 0$). This determines the inseparability of the cavity fields a_1 and a_3 . In a word, by the concurrent interactions, three cavity field become fully inseparable.

It is hard to give the exact conditions for the normalized detunings $\delta_{1,2}$ under which entanglement is existent. We can make a rough estimate of the parameters for entanglement. First, we note that no entanglement occurs when $\delta_1 = 0$ and/or $\delta_2 = 0$, i.e., when either or both

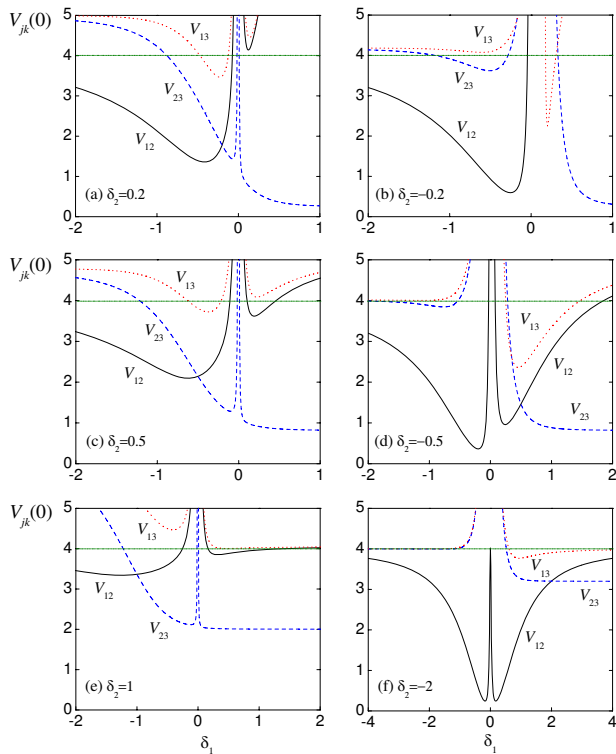


FIG. 4: (Color online) The output zero frequency spectra $V_{jk}(0)$ as functions of normalized detuning δ_1 for (a,b) $\delta_2 = \pm 0.2$, (c,d) $\delta_2 = \pm 0.5$, (e) $\delta_2 = 1$, and (f) $\delta_2 = -2$. The other parameters are listed in the text. Any two of the correlations falling below 4 are sufficient to demonstrate that genuine tripartite entanglement is present.

of the driving fields are resonant with the atoms. When $\delta_j = 0$ ($j = 1, 2$) we have $c_j^2 = s_j^2 = \frac{1}{2}$, $P_j^+ = P_j^- = \frac{1}{2}$, which correspond to $\tilde{\lambda}_1 = -\frac{\kappa_1}{2}$, $\tilde{\chi}_{12} = 0$ for $j = 1$ and $\tilde{\lambda}_3 = -\frac{\kappa_3}{2}$, $\tilde{\chi}_{23} = 0$ for $j = 2$. We see from Eq. (12) that once on resonance, a_1 and/or a_3 are only damped by the vacuum reservoir, but not amplified by any mechanism, let alone the cross coupling between a_1 and a_2 and/or the coupling between a_2 and a_3 [42, 43]. Therefore, tripartite entanglement appears only when the driving fields are off resonance with the atomic transitions. Similarly, the detunings are required for the related schemes, such as the double Lambda schemes [20, 21], where no entanglement occurs on exact double resonances, as was pointed out in Ref. [21].

Second, the entanglement criteria are well satisfied for the present scheme when the two normalized detunings $\delta_{1,2}$ have the opposite signs. This is referred to as a characteristic feature as above. In order to show this feature clearly, we plot the output zero frequency spectra $V_{12}(0)$, $V_{23}(0)$, and $V_{13}(0)$ in Fig. 6 for various ratios of the normalized detunings: (a) $\delta_2 = -\frac{1}{3}\delta_1$, (b) $\delta_2 = -\frac{1}{2}\delta_1$, (c) $\delta_2 = -\delta_1$, (d) $\delta_2 = -2\delta_1$, (e) $\delta_2 = -3\delta_1$, (f) $\delta_2 = -4\delta_1$. Let us examine first the right wing ($\delta_1 > 0$). Any two of these three curves dropping below 4 are

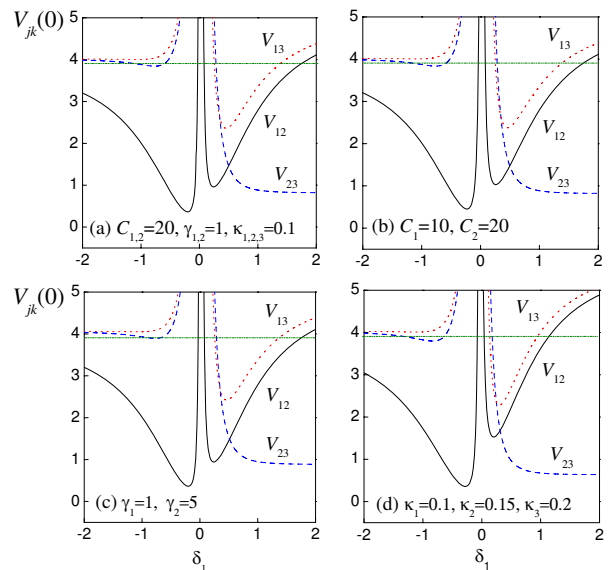


FIG. 5: (Color online) The output zero frequency spectra $V_{jk}(0)$ as functions of normalized detuning δ_1 for (a) the same parameters as in Fig. 4(d), (b) different cooperativity parameters $C_1 = 10$, $C_2 = 20$, (c) different atomic decay rates $\gamma_1 = 1$, $\gamma_2 = 5$, and (d) different cavity loss rates $\kappa_1 = 0.1$, $\kappa_2 = 0.15$, $\kappa_3 = 0.2$. In (b,c,d), the other parameters are the same as in (a).

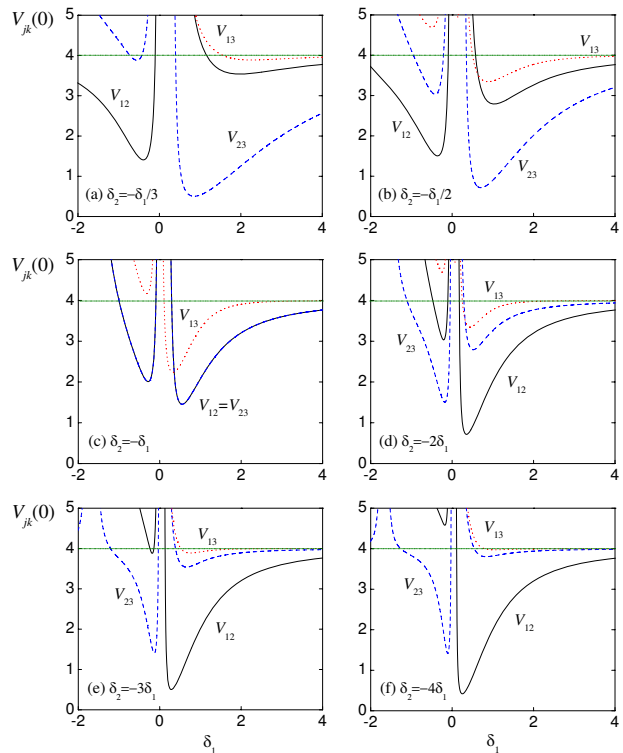


FIG. 6: (Color online) The output zero frequency spectra $V_{jk}(0)$ as functions of normalized detuning δ_1 for (a) $\delta_2 = -\frac{1}{3}\delta_1$, (b) $\delta_2 = -\frac{1}{2}\delta_1$, (c) $\delta_2 = -\delta_1$, (d) $\delta_2 = -2\delta_1$, (e) $\delta_2 = -3\delta_1$, (f) $\delta_2 = -4\delta_1$.

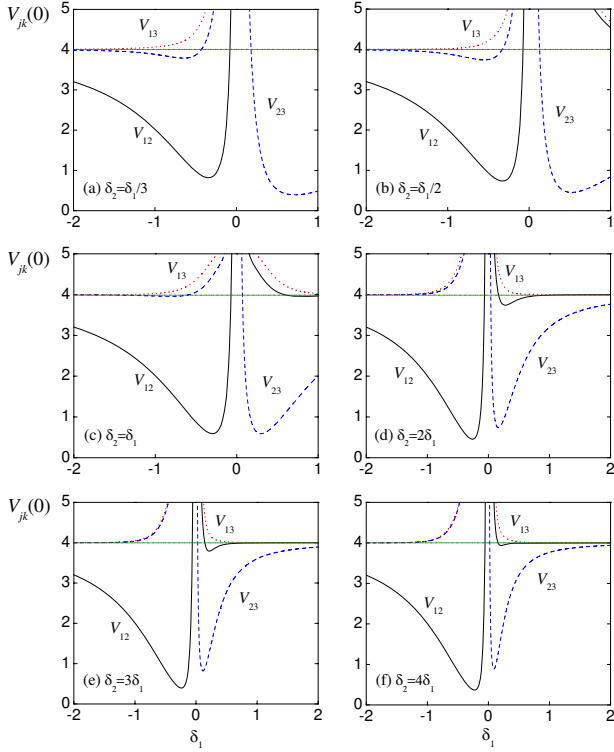


FIG. 7: (Color online) The output zero frequency spectra $V_{jk}(0)$ as functions of normalized detuning δ_1 for (a) $\delta_2 = \frac{1}{3}\delta_1$, (b) $\delta_2 = \frac{1}{2}\delta_1$, (c) $\delta_2 = \delta_1$, (d) $\delta_2 = 2\delta_1$, (e) $\delta_2 = 3\delta_1$, (f) $\delta_2 = 4\delta_1$.

sufficient for tripartite GHZ entanglement. Indeed, for various cases, there is a range where there are at least two curves falling below 4. For $\delta_2 = -\delta_1$, the curves V_{12} and V_{23} coincide and both fall below 4 when $\delta_1 > 0.1$. As the ratio $\frac{\delta_2}{\delta_1}$ deviates from -1 , the minimal value of δ_1 for two correlations less than 4 rises slightly. For $\delta_2 = -\frac{1}{2}\delta_1$, both V_{13} and V_{23} are less than 4 when $\delta_1 > 0.5$, and for $\delta_2 = -\frac{1}{3}\delta_1$, both V_{12} and V_{23} are reduced below 4 when $\delta_1 > 1.16$. For $\delta_2 = -2\delta_1$, both V_{12} and V_{13} descend below 4 when $\delta_1 > 0.25$. For $\delta_2 = -3\delta_1$ and $\delta_2 = -4\delta_1$, both V_{12} and V_{23} are smaller than 4 when $\delta_1 > 0.38$ and $\delta_1 > 0.55$, respectively. For various cases, all correlations approach 4 when δ_1 be large, i.e., when δ_1 approaches 4. This is because the atom-field interactions become so weak for the large detunings. Roughly, we have the range of the normalized detunings for entanglement in the $\delta_1 > 0$ wing

$$-3 \lesssim \frac{\delta_2}{\delta_1} \lesssim -\frac{1}{3}, \quad z_1 \lesssim (\delta_1, -\delta_2) \lesssim 4, \quad (19)$$

where $0.1 \lesssim z_1 \lesssim 1.16$, and the parameter z_1 has the minimal value 0.1 for $\frac{\delta_2}{\delta_1} = -1$, and becomes large as $\frac{\delta_2}{\delta_1}$ deviates from -1 . Then let us turn to the left wing ($\delta_1 < 0$). We can see a limited range where the curves V_{12} and V_{23} fall below 4. For $\frac{\delta_2}{\delta_1} = -1$, the curves V_{12} and V_{23} are identical and fall below 4 in the range of

$\delta_1 \sim (-1, -0.1)$. As the ratio $\frac{\delta_2}{\delta_1}$ deviates from -1 , the range of δ_1 for entanglement becomes narrow. For $\delta_2 = -\frac{1}{2}\delta_1$ and $\delta_2 = -2\delta_1$, both V_{12} and V_{23} are less than 4 in the regions of $\delta_1 \sim (-0.95, -0.21)$ and $(-0.47, -0.11)$, respectively. Roughly, we have the limited range of the normalized detunings for entanglement in the $\delta_1 < 0$ wing

$$-2 \lesssim \frac{\delta_2}{\delta_1} \lesssim -\frac{1}{2}, \quad z_2 \lesssim (\delta_1, -\delta_2) \lesssim z_3, \quad (20)$$

where $-1 \lesssim z_2 \lesssim 0.47$, $-0.21 \lesssim z_3 \lesssim -0.1$, and the parameter z_2 (z_3) has minimal (maximal) value -1 (-0.1) when $\frac{\delta_2}{\delta_1} = -1$ and rises (falls) as $\frac{\delta_2}{\delta_1}$ deviates from -1 .

Thirdly, as a comparison, we find that the entanglement criteria are not well satisfied when the normalized detunings $\delta_{1,2}$ have the same signs. In this case, we show the output zero frequency correlations in Fig. 7 for (a) $\delta_2 = \frac{1}{3}\delta_1$, (b) $\delta_2 = \frac{1}{2}\delta_1$, (c) $\delta_2 = \delta_1$, (d) $\delta_2 = 2\delta_1$, (e) $\delta_2 = 3\delta_1$, (f) $\delta_2 = 4\delta_1$. This figure shows that when $0 < \frac{\delta_2}{\delta_1} < 1$, there is a narrow region in the left wing, where both V_{12} and V_{23} are below 4. Such a narrow region is transferred to the right wing when $\frac{\delta_2}{\delta_1} > 1$. In both cases, however, either V_{23} or V_{12} is just a little slightly below 4. This indicates that the entanglement criteria are not so well satisfied even in such a narrow region when the normalized detunings have the same signs. The remarkable difference has its physical origin. We see from the middle equation of Eq. (12) that the modes $a_{1,3}$ are coupled to the mode a_2 through the cross coupling coefficients $-\tilde{\chi}_{12}$ and $\tilde{\chi}_{23}$, respectively, where the minus sign means an extra phase difference π . When $\delta_{1,2}$ have the same signs, so do $\tilde{\chi}_{12}$ and $\tilde{\chi}_{23}$. This determines that the interactions of $a_{1,3}$ with a_2 have the opposite roles. It is not difficult to understand that the detunings of the same signs are not so suitable for creating entanglement. The case is reversed for the detunings of the opposite signs. When $\delta_{1,2}$ have the opposite signs, so do $\tilde{\chi}_{12}$ and $\tilde{\chi}_{23}$, which instead indicates that the fields $a_{1,3}$ are coupled to a_2 with the same phase. By comparison, as a rough estimate, Eqs. (19,20) turn out to be good conditions for tripartite GHZ entanglement in the present scheme.

IV. REALISTIC CONSIDERATIONS

So far we have shown the quantum correlations by considering zero-temperature environment and neglecting the driving field linewidths. At nonzero temperature the bath has nonzero thermal photons. Then we should include the effects of thermal photons [46]. The average number of thermal photons of frequency ω_T is $\bar{n}(\omega_T) = [\exp(\hbar\omega_T/kT) - 1]^{-1}$, where k is the Boltzmann constant and T is the thermal bath temperature. At room temperature ($T = 300$ K), $\lambda \approx 50$ μm , $\omega_T \approx 6 \times 10^{12}$ Hz correspond to $\hbar\omega_T/kT = 1$. For $\omega_T \gg 6 \times 10^{12}$ Hz, $\bar{n}(\omega_T) \rightarrow 0$. For example, $\lambda = 620.1$ nm, $\omega_T = 2\pi \times 4.838 \times 10^{14}$ Hz, we have $\hbar\omega_T \approx 2$ eV, which is much larger than the room temperature energy, $kT \approx \frac{1}{40}$ eV. This corresponds to a negligible average

number of thermal photons $\bar{n} \approx e^{-80} \approx 0$. In this case the thermal reservoir has a negligible effect. If ω_T is comparable to 6×10^{12} Hz, for example, $\lambda = 2 \times 10^4$ nm, $\omega_T = 2\pi \times 1.5 \times 10^{13}$ Hz, we have the average thermal photon number of $\bar{n} = 0.1$. In such a situation, the thermal reservoir effect has to be included. According to the standard reservoir theory [46], we add to Eq. (5) the additional term

On the other hand, the applied driving fields usually have the fluctuating phases, which correspond to finite bandwidths [40]. We assume $\Phi_j(t)$ to be the fluctuating phases associated with Rabi frequencies Ω_j . These fluctuations are characterized by the random forces $\dot{\Phi}_j(t) = \chi_j(t)$ with zero averages and the white noise correlations [46]: $\langle \chi_j(t) \rangle = 0$ and $\langle \chi_j(t) \chi_j(t') \rangle = \gamma_{D_j} \delta(t - t')$, where γ_{D_j} are the linewidths of the laser fields Ω_j . In this case we add to Eq. (4) an additional atomic damping term

$$\mathcal{L}'_a \rho = \sum_{j=1}^2 \sum_{\mu_j=1}^{N_j} \frac{\gamma_{D_j}}{4} \mathcal{D}[\sigma_{11}^{\mu_j} - \sigma_{00}^{\mu_j}] \rho. \quad (21)$$

Using the unitary transformations in Eq. (6), we rewrite the additional term as

$$\begin{aligned} \mathcal{L}'_a \rho = & \sum_{j=1}^2 \sum_{\mu_j=1}^{N_j} \frac{\gamma_{D_j}}{4} \{ 4c_j^2 s_j^2 (\mathcal{D}[\sigma_{+-}^{\mu_j}] \rho + \mathcal{D}[\sigma_{-+}^{\mu_j}] \rho) \\ & + (c_j^2 - s_j^2)^2 \mathcal{D}[\sigma_{++}^{\mu_j} - \sigma_{--}^{\mu_j}] \rho \}. \end{aligned} \quad (22)$$

The equation for the dressed populations P_j^\pm is changed as

$$\dot{P}_j^+ = \gamma_j s_j^4 P_j^- - \gamma_j c_j^4 P_j^+ + 2\gamma_{D_j} c_j^2 s_j^2 (P_j^- - P_j^+), \quad (23)$$

together with the closure relation $P_j^+ + P_j^- = 1$. At the steady state we obtain the dressed populations

$$\begin{aligned} P_j^+ &= \frac{\gamma_j s_j^4 + 2\gamma_{D_j} c_j^2 s_j^2}{\gamma_j (c_j^4 + s_j^4) + 4\gamma_{D_j} c_j^2 s_j^2}, \\ P_j^- &= \frac{\gamma_j c_j^4 + 2\gamma_{D_j} c_j^2 s_j^2}{\gamma_j (c_j^4 + s_j^4) + 4\gamma_{D_j} c_j^2 s_j^2}. \end{aligned} \quad (24)$$

$$\mathcal{L}'_c \rho = \sum_{l=1}^3 \frac{\kappa_l \bar{n}_l}{2} (\mathcal{D}[a_l] \rho + \mathcal{D}[a_l^\dagger] \rho). \quad (25)$$

Taking into account the change in the dressed populations and changing the parameters in Eq. (11) as $\lambda_l \rightarrow \lambda_l + \kappa_l \bar{n}_l$, $\xi_l \rightarrow \xi_l + \kappa_l \bar{n}_l$ ($l = 1, 2, 3$) together with $\Gamma_j \rightarrow \Gamma_j + \gamma_{D_j} (c_j^4 + s_j^4)$ ($j = 1, 2$), we obtain the master equation for the cavity fields. Again we can follow the same steps as above to give the correlations. For simplicity, we assume that the a_l modes have the same average thermal photons numbers $\bar{n}_l = \bar{n}$, and that the driving fields have the same linewidths $\gamma_{D_j} = \gamma_D$. The effects of the realistic factors on the quantum correlations are presented in Fig. 8 and Fig. 9. Figure 8 shows

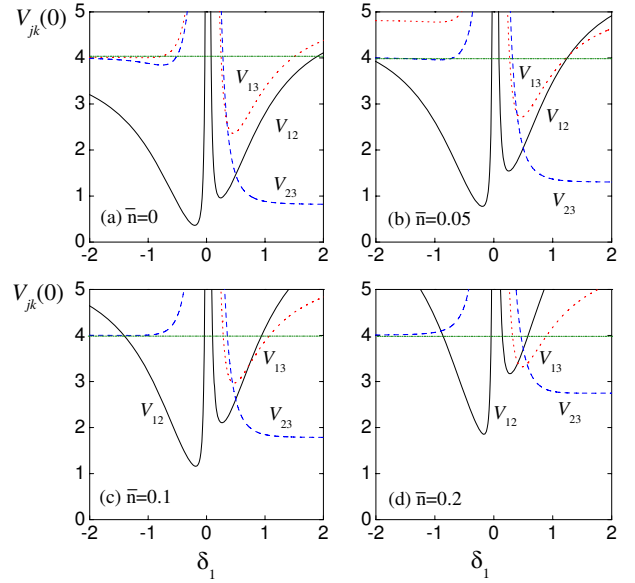


FIG. 8: (Color online) The output zero frequency spectra $V_{jk}(0)$ as functions of normalized detuning δ_1 for different numbers of the thermal photons: (a) $\bar{n} = 0.0$, (b) $\bar{n} = 0.05$, (c) $\bar{n} = 0.1$, and (d) $\bar{n} = 0.2$. The other parameters are $\gamma_D = 0$ and those as in Fig. 4(d).

the effects of the thermal photons. The parameters are (a) $\bar{n} = 0$, (b) $\bar{n} = 0.05$, (c) $\bar{n} = 0.1$, and (d) $\bar{n} = 0.2$. The other parameters are $\gamma_D = 0$ and those as in Fig. 4(d). It is clear that the thermal photons lead to significant reduction of correlation. With increasing numbers of the thermal photons, the correlation spectra are further suppressed. However, even for $\bar{n} = 0.2$, we have good entanglement. In figure 9 we show the effects of the driving field linewidths for (a) $\gamma_D = 0$, (b) $\gamma_D = 0.25$, (c) $\gamma_D = 0.5$, and (d) $\gamma_D = 1$. The other parameters are $\bar{n} = 0$ and those as in Fig. 4(d). Although the linewidth varies from $\gamma_D = 0$ to $\gamma_D = 1$, the correlation spectra are not significantly changed. It shows clearly that the present scheme is robust against the thermal fluctuations and the laser linewidths.

For the experimental realization, the present scheme is accessible in alkali atomic systems. In order to avoid the Doppler effect and to resolve the fine levels we use two ensembles of cold atoms [38, 39]. As an example, we can use Rubidium 87 D2 transition hyperfine structure for the atomic ensembles. We employ the $|5S_{1/2}, F = 2\rangle \leftrightarrow |5P_{3/2}, F' = 2\rangle$ transition for the first ensemble, and the second one uses the $|5S_{1/2}, F = 2\rangle \leftrightarrow |5P_{3/2}, F' = 3\rangle$ transition. Two transitions are separated from each other by 267 MHz. Two hyperfine levels $|5P_{3/2}, F' = 1\rangle$ and $|5P_{3/2}, F' = 0\rangle$ lies below the lower excited state by 157 MHz and 229 MHz, respectively. When Δ_1 is far less than 157 MHz, the two adjacent levels are far off resonances and the additional Stark shifts are negligibly small. Since $|5S_{1/2}, F = 1\rangle$ is below $|5S_{1/2}, F = 2\rangle$ by 6.8 GHz and $|5P_{3/2}, F' = 3\rangle$ is 267

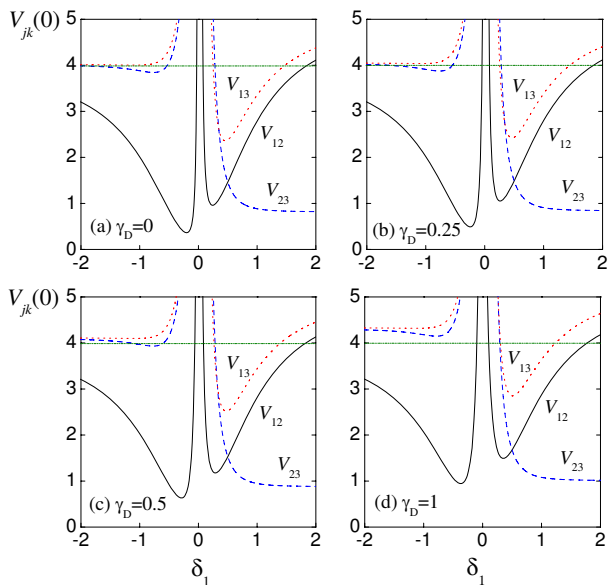


FIG. 9: (Color online) The output zero frequency spectra $V_{jk}(0)$ as functions of normalized detuning δ_1 for different driving field linewidths: (a) $\gamma_D = 0$, (b) $\gamma_D = 0.25$, (c) $\gamma_D = 0.5$, and (d) $\gamma_D = 1$. The other parameters are $\bar{n} = 0$ and those as in Fig. 4(d).

MHz above $|5P_{3/2}, F' = 2\rangle$, we can use the transition $|5S_{1/2}, F = 1\rangle \leftrightarrow |5P_{3/2}, F' = 0\rangle$ as a repumping transition.

Finally, it is interesting to compare the present system with the existing multilevel schemes, which are divided into three kinds in the introduction paragraph. The essence in common is to use the two-photon processes. The remarkable difference between them lies in that the two-photon processes are created in different circumstances. First, for the correlated emission laser schemes [19–21], the two-photon process is established by combining the EIT and Raman transitions in Lambda systems to form a loop of transitions. In the loop, two cavity fields are in the two-photon interactions, which occurs between the resonantly or near-resonantly coupled atomic levels. By such arrangements, the atomic coherence by the resonant or near-resonant driving is responsible for both the laser gain and the quantum entanglement. Second, for those schemes based on the parametric interactions [22, 23], the atoms are almost not excited and the field operators are isolated from the atomic operators. Through a loop of transitions, the involved cavity fields can be made to be in a two-photon interaction. However, the susceptibility is weak due to the fact that all fields, including the driving and cavity fields, are far off resonance with the atoms.

Our model belongs to the third kind of schemes, which are based on the wave-mixing interactions in near-resonant systems [27–35]. The common physics is to use the Rabi resonances to create the two-photon interactions and the quantum correlations between the cavity fields

[42, 43]. The essential difference of the present scheme from the previous ones lies in the structure of the dressed states [41]. Our system involves two-level atoms, the dressed states of which are in an infinite ladder of doublets. The dressed states of the same doublet can be sufficiently separated simply by increasing the driving field amplitude and/or the atom-field detuning. The most classical example is the Mollow structure of the resonance fluorescence spectrum [40–43]. The Rabi resonances are separated simply by the generalized Rabi frequency. In sharp comparison, the three- or more-level systems have an infinite cascade of triplets or more of dressed states. Within the same multiplets, the dressed states generally are not equally spaced unless all involved fields are resonant with respective transitions. More often than not, there are two or more that are spaced closely. In this case, the adjacent Rabi resonances are not easily separated from each other. Such examples were verified for the resonance fluorescence spectrum of an off-resonantly driven multilevel atom [47–49]. For the close Rabi resonances, it is difficult to choose and control frequencies of the cavity fields. Once a cavity field is coupled to adjacent dressed transitions, different transitions will play opposite effects on the quantum correlations. Clearly, this increases the difficulty in obtaining the desired quantum correlations. The above comparison shows clearly that it is advantageous to use a cascade of two-level atomic ensembles as in our scheme.

Another advantage lies in that the frequencies of the cavity fields can be controlled independently for the present two-level scheme but not for the multilevel schemes. As is well known, varying any driving field in multilevel systems will modify eigenvalues of all dressed states. In other words, all Rabi resonances change their frequencies so long as any driving field is varied. As a consequence, the frequencies of all the cavity fields from the Rabi resonances are modified due to the change in any driving field. However, the case differs completely for the present scheme. Different ensembles of atoms are separated from each other, each of which is driven by a different driving field. When we change the dressed states of one atomic ensemble, the dressed states of another atomic ensemble can be kept unchanged. Therefore, we can first fix the frequencies of the cavity fields $a_{1,2}$ as $\nu_{1,2} = \omega_1 \pm \sqrt{\Delta_1^2 + \Omega_1^2}$ by controlling the first driving field, and then adjust the frequency of the cavity field a_3 as $\nu_3 = \omega_2 + \sqrt{\Delta_2^2 + \Omega_2^2}$ by varying the second driving field. This can be generalized to more modes in the same way.

V. CONCLUSION

In summary, we have presented a scheme for three-mode interactions and GHZ entanglement. This scheme involves two atomic ensembles, each of which is driven by a single driving field. The concurrent interactions are established since the cavity field of the in-between

frequency is simultaneously coupled to the higher Rabi sideband of one ensemble and to the lower Rabi sideband of the other. It has been shown that GHZ entanglement is achievable for a wide range of parameters. Such a scheme is straightforwardly scalable when more atomic ensembles of close frequencies are included. This device can be used as a useful multipartite entangled resource for the CV quantum networks and information.

Acknowledgements

This work is supported by the National Natural Science Foundation of China (Grants No. 11074086 and 61178021), National Basic Research Program of China (Grant No. 2012CB921604), and Natural Science Foundation of Hubei Province (Grant No. 2010CDA075).

-
- [1] S. L. Braunstein and P. van Loock, *Rev. Mod. Phys.* **77**, 513 (2005).
- [2] L. Vaidman, *Phys. Rev. A* **49**, 1473 (1994).
- [3] S. L. Braunstein and H. J. Kimble, *Phys. Rev. Lett.* **80**, 869 (1998).
- [4] A. Furusawa, J. L. Sorensen, S. L. Braunstein, C. A. Fuchs, H. J. Kimble, and E. S. Polzik, *Science* **282**, 706 (1998).
- [5] S. L. Braunstein and H. J. Kimble, *Nature (London)* **394**, 840 (1998).
- [6] H. Yonezawa, T. Aoki, and A. Furusawa, *Nature (London)* **431**, 430 (2004).
- [7] X. Li, Q. Pan, J. Jing, J. Zhang, C. Xie, and K. Peng, *Phys. Rev. Lett.* **88**, 047904 (2002).
- [8] A. M. Lance, T. Symul, W. P. Bowen, B. C. Sanders, and P. K. Lam, *Phys. Rev. Lett.* **92**, 177903 (2004).
- [9] J. Jing, J. Zhang, Y. Yan, F. Zhao, C. Xie, and K. Peng, *Phys. Rev. Lett.* **90**, 167903 (2003).
- [10] T. Aoki, N. Takei, H. Yonezawa, K. Wakui, T. Hiraoka, A. Furusawa, and P. van Loock, *Phys. Rev. Lett.* **91**, 080404 (2003).
- [11] X. Su, A. Tan, X. Jia, J. Zhang, C. Xie, and K. Peng, *Phys. Rev. Lett.* **98**, 070502 (2007).
- [12] A. Furusawa and N. Takei, *Phys. Rep.* **443**, 97 (2007).
- [13] D. M. Greenberger, M. A. Horne, A. Shimony, and A. Zeilinger, *Am. J. Phys.* **58**, 1131 (1990).
- [14] S. E. Harris, *Phys. Today* **50** (7), 36 (1997).
- [15] J. P. Marangos, *J. Mod. Opt.* **45**, 471 (1998).
- [16] L. V. Hau, S. E. Harris, Z. Dutton, and C. H. Behroozi, *Nature (London)* **397**, 594 (1999).
- [17] M. D. Lukin and A. Imamoglu, *Nature (London)* **413**, 273 (2001); M. D. Lukin, *Rev. Mod. Phys.* **75**, 457 (2003).
- [18] M. Fleischhauer, A. Imamoglu, and J. P. Marangos, *Rev. Mod. Phys.* **77**, 633 (2005).
- [19] H. Xiong, M. O. Scully, and M. S. Zubairy, *Phys. Rev. Lett.* **94**, 023601 (2005).
- [20] M. Kiffner, M. S. Zubairy, J. Evers, and C. H. Keitel, *Phys. Rev. A* **75**, 033816 (2007).
- [21] C. H. Raymond Ooi, *Phys. Rev. A* **76**, 013809 (2007).
- [22] M. D. Reid, D. F. Walls, and B. J. Dalton, *Phys. Rev. Lett.* **55**, 1288 (1985).
- [23] R. Guzmán, J. C. Retamal, E. Solano, and N. Zagury, *Phys. Rev. Lett.* **96**, 010502 (2006).
- [24] A. Einstein, B. Podolsky, and N. Rosen, *Phys. Rev.* **47**, 777 (1935).
- [25] S. Pielawa, G. Morigi, D. Vitali, and L. Davidovich, *Phys. Rev. Lett.* **98**, 240401 (2007).
- [26] M. Ikram, G. X. Li, and M. S. Zubairy, *Phys. Rev. A* **76**, 042317 (2007).
- [27] Y. Wu and L. Deng, *Opt. Lett.* **29**, 1144 (2004); 2064 (2004).
- [28] X. Li and X. M. Hu, *Phys. Rev. A* **80**, 023815 (2009).
- [29] X. Y. Lu, P. Huang, W. X. Yang, and X. Yang, *Phys. Rev. A* **80**, 032305 (2009).
- [30] X. M. Hu, H. Sun, and F. Wang, *Phys. Rev. A* **82**, 045807 (2010).
- [31] X. Zhang and X. M. Hu, *Phys. Rev. A* **81**, 013811 (2010).
- [32] H. T. Tan and G. X. Li, *Phys. Rev. A* **82**, 032322 (2010).
- [33] W. X. Shi, X. M. Hu, J. Y. Li, and F. Wang, *J. Phys. B* **43**, 155506 (2010).
- [34] Y. B. Yu, J.T. Sheng, and M. Xiao, *Phys. Rev. A* **83**, 012321 (2011).
- [35] H. Sun and X. M. Hu, *J. Phys. B* **44**, 205504 (2011).
- [36] O. S. Mishina, A. S. Sheremet, N. V. Larionov, and D. V. Kupriyanov, *Opt. Spectrosc.* **108**, 313 (2010).
- [37] P. van Loock and A. Furusawa, *Phys. Rev. A* **67**, 052315 (2003).
- [38] V. Josse, A. Dantan, L. Vernac, A. Bramati, M. Pinard, and E. Giacobino, *Phys. Rev. Lett.* **91**, 103601 (2003).
- [39] V. Josse, A. Dantan, A. Bramati, M. Pinard, and E. Giacobino, *Phys. Rev. Lett.* **92**, 123601 (2004).
- [40] M. O. Scully and M. S. Zubairy, *Quantum Optics* (Cambridge University Press, Cambridge, England, 1997).
- [41] C. Cohen-Tannoudji, J. Dupont-Roc, and G. Grynberg, *Atom-Photon Interactions* (Wiley, New York, 1992).
- [42] R. W. Boyd, *Nonlinear Optics* (Academic Press, Boston, 1992).
- [43] P. Meystre and M. Sargent III, *Elements of Quantum Optics* (Springer-Verlag, Berlin, 1991).
- [44] C. W. Gardiner and P. Zoller, *Quantum Noise*, 2nd ed. (Springer, Berlin, 2000).
- [45] P. D. Drummond and C. W. Gardiner, *J. Phys. A: Math. Gen.* **13**, 2353 (1980); P. D. Drummond and D. F. Walls, *Phys. Rev. A* **23**, 2563 (1981).
- [46] M. Sargent III, M. O. Scully, and W. E. Lamb, Jr., *Laser Physics* (Addison-Wesley, Reading, MA, 1974), pp. 327.
- [47] C. Cohen-Tannoudji and S. Reynaud, *J. Phys. B: At. Mol. Phys.* **10**, 345; 365; 2311 (1977).
- [48] S. V. Lawande, Richard D'Souza, and R. R. Puri, *Phys. Rev. A* **36**, 3228 (1987); A. S. Jayarao, S. V. Lawande, and R. D'Souza, *Phys. Rev. A* **39**, 3464 (1989).
- [49] L. M. Narducci and M. O. Scully, G. L. Oppo, P. Ru, and J. R. Tredicce, *Phys. Rev. A* **42**, 1630 (1990).